Selected Paper

[{RhCl(CO)$_2$}$_2$]-Derived MCM-41-Tethered Rhodium Complex Catalysts via Phosphine, Amine and Thiol Ligands for Cyclohexene Hydroformylation

Lin Huang and Sibudjing Kawi*

Department of Chemical and Environmental Engineering, and Chemical and Process Engineering Centre, National University of Singapore, 10 Kent Ridge Crescent, Singapore 119260

Received June 23, 2003; E-mail: chekawis@nus.edu.sg

Functionalized silicate MCM-41-tethered rhodium complexes derived from [{RhCl(CO)$_2$}$_2$] have been studied by infrared spectroscopy (IR), X-ray diffraction (XRD) and N_2 adsorption–desorption. [{RhCl(CO)$_2$}$_2$] reacts with aminated MCM-41 to result in a splitting of the chloride bridge. The same result is presumed with phosphinated MCM-41. Thiolated MCM-41 is presumed to displace the chloride in the bridge with thiol ligands. The tethering of rhodium complexes to MCM-41 leads to reduced pore sizes, pore volumes and BET surface areas without altering the structural ordering of MCM-41. The MCM-41-tethered catalysts show distinct activities and resistance to rhodium leaching in cyclohexene hydroformylation under equimolar CO and H_2 at 28 bar and 100 °C, depending on the nature of complexation of the supported donor ligands with the rhodium centre. The aminated MCM-41-tethered catalyst displays good activity, selectivity and recycling for the formation of cyclohexane carboxaldehyde. The mesoporous structure of MCM-41 remains stable during the reaction.

The immobilization of metallic and organometallic complex catalysts is viewed as an important and practical issue for the separation and recycling of catalysts in the industrial reaction processes. The preparation of heterogeneous hydroformylation catalysts has made wide use of various supports such as organic polymers, SiO_2, Al_2O_3, MgO, ZnO, clays, active carbons and zeolites.[1] Although zeolites provide an excellent catalyst support with high surface area and unusual catalytic properties, their applications in catalysis are limited by their relatively small pore openings.

The discovery of the first mesoporous molecular sieve, MCM-41, by Mobil's researchers in 1991–92, opened up the opportunities to apply ordered mesoporous materials to the field of catalysis. Besides its high surface area (>700 m^2/g), MCM-41 possesses a hexagonal arrangement of highly uniform sized mesopores (15 to 100 Å). The high surface area allows for the immobilization of large amounts of catalytic components. The large pore size makes shape-selective conversions of bulky molecules possible in the upgrading of heavy residues in refineries and in the manufacture of fine chemicals. MCM-41-based catalysts have shown higher performances in several reactions such as alkylation, cracking, epoxidation, and NO_X selective reduction than conventional zeolite- and oxide-based catalysts.[2,3]

[{RhCl(CO)$_2$}$_2$] has been most commonly used as an organo-rhodium catalyst precursor to prepare organic polymer- and inorganic oxide-tethered rhodium complexes via different donor ligands.[4–15] Some of these tethered rhodium complexes have been investigated in olefin hydroformylation.[5–7,9–11,14,16] However, there have been very few papers about the catalytic application of MCM-41 in hydroformylation.[17] The mesoporous framework of MCM-41 is not only freely accessible to large reactant molecules, but favors tethering large amounts of metallic complexes.

In this paper, we describe the preparative processes of rhodium complexes tethered to MCM-41 from [{RhCl(CO)$_2$}$_2$] by use of phosphine, amine, and thiol ligands. For the first time, we deal with the catalytic results of these MCM-41-tethered catalysts in cyclohexene hydroformylation and the effects of donor ligands on the catalytic activity and stability.

Experimental

Sodium silicate solution (25.5–28.5% SiO_2, 7.5–8.5% Na_2O), cetyl trimethylammonium bromide (CTMABr, 98–101%) and cyclohexene (99%) were purchased from Merck. Tetraethylammonium hydroxide solution (TEAOH, 20%) was obtained from Sigma. (3-Chloropropyl)trimethoxysilane ([{Cl(CH$_2$)$_3$}Si(OMe)$_3$], 97%), (3-aminopropyl)triethoxysilane ([{H$_2$N(CH$_2$)$_3$}Si(OEt)$_3$], 99%), (3-mercaptopropyl)trimethoxysilane ([{HS(CH$_2$)$_3$}Si(OMe)$_3$], 96%) and potassium diphenylphosphide ($KPPh_2$, 0.5 M solution in tetrahydrofuran (THF)) were supplied by Aldrich. Dicarbonylchlororhodium(I) dimer ([{RhCl(CO)$_2$}$_2$]) was supplied by Strem. All other reagents were purchased commercially. Organic solvents were distilled and dried prior to use. The gases CO + H_2 and N_2 had a purity of 99.999%.

Silicate MCM-41 was synthesized as described below. 79.6 g of sodium silicate solution and 50 g of distilled water were added to a solution containing 64.4 g of CTMABr and 130 mL of TEAOH. After stirring for 10 min to form a gel, 1 M H_2SO_4 was added to the gel and the pH value adjusted to 9.5–10. Additional water was added to make the following molar ratio of the final gel composition: 1.0 SiO_2:0.48 CTMABr:0.48 TEAOH:0.39 Na_2O:50 H_2O. The gel mixture was stirred for 2 h at room temperature, transferred into a polypropylene bottle and then statically heated

Published on the web February 10, 2004; DOI 10.1246/bcsj.77.295

at 96 °C for 4 days under autogenerated pressure. The final solid material obtained was filtered off, washed with distilled water until free of bromide ions, dried and calcined in an oven at 560 °C for 10 h. In order to regenerate sufficient amounts of OH groups on the MCM-41 surface, the calcined MCM-41 was exposed to air at room temperature for 2 days followed by dehydration at 200 °C for 5 h.

To functionalize silicate MCM-41, 10 mL of organosilane was mixed with 2.0 g of MCM-41 in 150 mL of toluene. The mixture was refluxed under N_2 for 16 h. The resulting solid was filtered off, washed with 200 mL of chloroform and dried under vacuum. The chlorinated, aminated, and thiolated MCM-41 samples thus prepared contained 5.5% Cl, 3.7% N, and 5.0% S, respectively. The chlorinated MCM-41 was further refluxed with 1 mL of $KPPh_2$ in 25 mL of THF under N_2 for 1 h. After filtration, washing with 100 mL of methanol and drying under vaccum, the resulting phosphinated MCM-41 contained 0.2% Cl and 4.0% P. Chlorinated, phosphinated, aminated, and thiolated MCM-41 samples are denoted as MCM-41(Cl), MCM-41(PPh_2), MCM-41(NH_2), and MCM-41(SH), respectively.

Supported catalyst precursors were prepared as follows. 1.0 g of unfunctionalized or functionalized support was impregnated with a solution of [{RhCl(CO)$_2$}$_2$] (38 mg) in *n*-hexane under N_2. The system was stirred at room temperature under N_2 for 5 h. In the case of unfunctionalized MCM-41, the solid powder turned yellow in color and the yellow color of the solution remained unchanged at the end of stirring. In the case of functionalized MCM-41, the solid powder colorated and the yellow solution became colorless rapidly after stirring. MCM-41(PPh_2), MCM-41(NH_2), and MCM-41(SH) turned brown, yellow, and yellow in color, respectively after reacting with [{RhCl(CO)$_2$}$_2$]. Afterward, the liquid was drawn off with a syringe under N_2, and the resulting solid was washed three times with *n*-hexane under N_2 followed by drying under vacuum (10^{-2} Torr).

Hydroformylation of cyclohexene was conducted under 28 bar of an equimolar CO and H_2 mixture at 100 °C in an autoclave. 300 mg of catalyst precursor, 12 mL of cyclohexene and 55 mL of THF were first transferred to the autoclave inside a glove box. Subsequently, the CO + H_2 mixture was admitted after the reaction system had been purged with this reaction gas mixture. Sampling of the reaction mixture was done during the course of reaction. The samples were analyzed by gas chromatography.

IR experiments were carried out on a Shimadzu 8700 FTIR spectrometer at a resolution of 4 cm^{-1}. The solid samples studied were pressed into wafers of 15 mg each and placed in a single beam IR cell where the wafers could be subjected to the desired treatments. In situ IR studies of the reactivities between [{RhCl(CO)$_2$}$_2$] and unfunctionalized or functionalized MCM-41 were performed by dripping [{RhCl(CO)$_2$}$_2$] solution on unfunctionalized or functionalized MCM-41 wafers under N_2. IR spectra of supported rhodium complexes were recorded by subtracting the support contribution.

XRD of unfunctionalized and functionalized MCM-41 was performed on a Shimadzu XRD-6000 spectrometer with Cu Kα monochromatic radiation. N_2 adsorption–desorption experiments were done on a Quantachrome Autosorb-1 (AS-1) analyzer. The rhodium contents of the samples were determined by atomic absorption spectroscopy. The chlorine, sulfur, and phosphorus contents of the samples were analyzed by X-ray fluorescence. Thermogravimetric analysis (TGA) was used to estimate the contents of chlorine, nitrogen, and sulfur in MCM-41(Cl), MCM-41(NH_2), and MCM-41(SH).

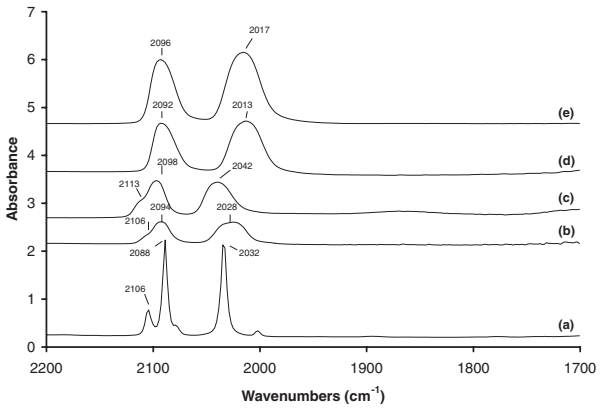

Fig. 1. IR spectra of (a) [{RhCl(CO)$_2$}$_2$]/*n*-hexane; (b) immediately after impregnation of MCM-41 with [{RhCl(CO)$_2$}$_2$]/*n*-hexane under N_2; (c) [{RhCl(CO)$_2$}$_2$]/MCM-41 after treatment under vacuum (10^{-5} Torr) for 1 h; (d) immediately after impregnation of MCM-41(NH_2) with [{RhCl(CO)$_2$}$_2$]/*n*-hexane under N_2; (e) [{RhCl(CO)$_2$}$_2$]/MCM-41(NH_2) after treatment under vacuum (10^{-5} Torr) for 1 h.

Results and Discussion

1. Studies of the Preparative Processes of MCM-41-Tethered Rhodium Complexes. (a) By IR Spectroscopy: Figure 1 shows the IR spectra during the impregnation of [{RhCl(CO)$_2$}$_2$] on the surfaces of MCM-41 and MCM-41(NH_2). When a yellow *n*-hexane solution of [{RhCl(CO)$_2$}$_2$] was dripped under N_2 onto a wafer of MCM-41 predehydrated at 200 °C in the IR cell, the wafer color turned yellow and the surface IR spectrum exhibited two broad carbonyl bands at 2094 and 2028 cm^{-1} and a shoulder near 2106 cm^{-1}. After removal of the solvent, the bands increased in intensity and shifted upward slightly. The relative band positions observed in Figs. 1(b) and 1(c) matched with that of [{RhCl(CO)$_2$}$_2$] in *n*-hexane shown in Fig. 1(a). In a separate impregnation experiment involving the powder sample depicted in the experimental section, the solution color still remained yellow, although the color of the solid turned yellow after stirring for 2 h in an *n*-hexane solution of [{RhCl(CO)$_2$}$_2$] with the MCM-41 powder.

The above observations assume that [{RhCl(CO)$_2$}$_2$] only physisorbs on the MCM-41 surface without chemical interaction, consistent with the known behavior of [{RhCl(CO)$_2$}$_2$] on the SiO_2 surface.[18]

As soon as a wafer of MCM-41(NH_2) predehydrated at 200 °C was impregnated with an *n*-hexane solution of [{RhCl(CO)$_2$}$_2$] under N_2, the wafer color turned yellow and the surface spectrum exhibited two broad carbonyl bands at 2092 and 2013 cm^{-1}. After evacuation of the solvent, the two bands shifted slightly upward. Their relative position differs from that of the 2098 and 2042 cm^{-1} bands for [{RhCl(CO)$_2$}$_2$] supported on MCM-41. Above all, it was noted that a shoulder did not appear near 2106 cm^{-1} simultaneously. In a parallel impregnation experiment involving the powder sample stated in the experimental part, the solid turned yellow in color while the solution became colorless upon mixing the MCM-41(NH_2) powder with the [{RhCl(CO)$_2$}$_2$] solution.

The results indicate that a chemical reaction between

$[\{RhCl(CO)_2\}_2]$ and the supported amine occurs. The presence of the monorhodium gem-dicarbonyl bands at 2092 and 2013 cm^{-1} explicitly demonstrates that the reaction of $[\{RhCl(CO)_2\}_2]$ with MCM-41(NH_2) results in a splitting of the chloride bridge with the formation of MCM-41{NH_2*cis*-$RhCl(CO)_2$}:

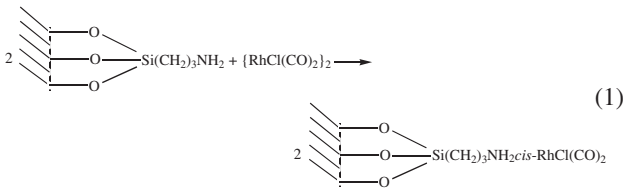

(1)

This chemistry coincides with that occurring on the $SiO_2(NH_2)$ surface.[4]

Although it is generally accepted that the reactions of $[\{RhCl(CO)_2\}_2]$ with nitrogen donor ligands generally lead to the splitting of the chloride bridge,[4,19–21] the production of $\{(EtO)_3Si(CH_2)_3NH_2ClRh(CO)_2\}$ is justified only by the reaction of $[\{RhCl(CO)_2\}_2]$ with 2 equiv of $[\{H_2N(CH_2)_3\}Si(OEt)_3]$ or less. As a matter of fact, $[\{H_2N(CH_2)_3\}Si(OEt)_3]$ (1.2×10^{-4} mol) was added dropwise to an *n*-hexane solution of $[\{RhCl(CO)_2\}_2]$ (6.0×10^{-5} mol) while stirring under N_2. The solution color changed from light yellow to deep yellow immediately. The spectrum of the reaction mixture displayed carbonyl bands at 2084, 2013sh, and 2003 cm^{-1} as shown in Fig. 2(a). This spectrum may be regarded as the superimposition of two pairs of bands at 2084 and 2013 cm^{-1}, and at 2084 and 2003 cm^{-1}. The 2084 and 2013 cm^{-1} bands can be assigned to $\{(EtO)_3Si(CH_2)_3NH_2$*cis*-$RhCl(CO)_2\}$. The 2084 and 2003 cm^{-1} bands can be attributed to $\{(EtO)_3Si(CH_2)_3NH_2$*trans*-$RhCl(CO)_2\}$. The 2013 cm^{-1} shoulder band depleted gradually together with the 2084 cm^{-1} band with increasing reaction time. The spectrum of the reaction mixture after 45 min consisted predominantly of the bands for $\{(EtO)_3Si(CH_2)_3NH_2$*trans*-$RhCl(CO)_2\}$, as shown in Fig. 2(b). When $[\{RhCl(CO)_2\}_2]$ (5.6×10^{-5} mol) was allowed to react with 4 equiv of $[\{H_2N(CH_2)_3\}Si(OEt)_3]$ (2.2×10^{-4} mol) under equivalent conditions, the solution color changed from light yellow to brown. The spectrum of the reaction mixture after 45 min exhibited an extra carbonyl band at 1949 cm^{-1} apart from the gem-dicarbonyl bands at 2081 and 2001 cm^{-1} which are attributed to $\{(EtO)_3Si(CH_2)_3NH_2$*trans*-$RhCl(CO)_2\}$. As the reaction proceeded, the 1949 cm^{-1} band developed at the expense of the 2081 and 2001 cm^{-1} band intensities, as shown in Figs. 2(c) and 2(d). This suggests that $\{(EtO)_3Si(CH_2)_3NH_2$*trans*-$RhCl(CO)_2\}$ arising from $[\{RhCl(CO)_2\}_2]$ is transformed to a *cis*-rhodium monocarbonyl complex under the action of another amine:

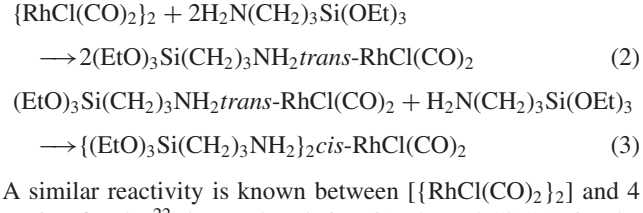

A similar reactivity is known between $[\{RhCl(CO)_2\}_2]$ and 4 equiv of PPh_3,[22] the product being $\{(PPh_3)_2RhCl(CO)_2\}$. The reaction vigorously takes place and is nearly complete within 5 min.[22] In contrast, the reaction between $[\{RhCl(CO)_2\}_2]$ and 4 equiv of $[\{H_2N(CH_2)_3\}Si(OEt)_3]$ proceeds slowly, as indicated by the IR spectral evolution.

The surface chemistry of $[\{RhCl(CO)_2\}_2]$ on MCM-41(NH_2) is consistent with the reactivity of $[\{RhCl(CO)_2\}_2]$ with 2 equiv of $[\{H_2N(CH_2)_3\}Si(OEt)_3]$ in solution. The *trans*-monorhodium isomer is preferentially formed in solution, and the *cis*-monorhodium isomer is favorably produced on the surface. This result further illustrates that the simple and desired reaction of a complex can be realized with a supported ligand on the surface. The reaction of $[\{RhCl(CO)_2\}_2]$ with $SiO_2(PPh_2)$ has also proven to produce $SiO_2\{PPh_2$*cis*-$RhCl(CO)_2\}$ with no carbonyl substitution.[4]

We did not pursue analogous IR studies on the reactivities of $[\{RhCl(CO)_2\}_2]$ with MCM-41(PPh_2) and with MCM-41(SH). The reactivities of $[\{RhCl(CO)_2\}_2]$ on $SiO_2(PPh_2)$ and on $SiO_2(SH)$ are well known.[4] The fact that the reactivities of $[\{RhCl(CO)_2\}_2]$ with MCM-41 and with MCM-41(NH_2) are identical with those of $[\{RhCl(CO)_2\}_2]$ with SiO_2 and with $SiO_2(NH_2)$ clearly shows that the surfaces of silicate MCM-41 and SiO_2 have the same chemical properties. Thus, we believe that the reaction results of $[\{RhCl(CO)_2\}_2]$ on $SiO_2(PPh_2)$ and on $SiO_2(SH)$ can apply to silicate MCM-41(PPh_2) and silicate MCM-41(SH). Namely, $[\{RhCl(CO)_2\}_2]$ and MCM-41(PPh_2) form MCM-41{PPh_2*cis*-$RhCl(CO)_2$} by splitting of the chloride bridge:

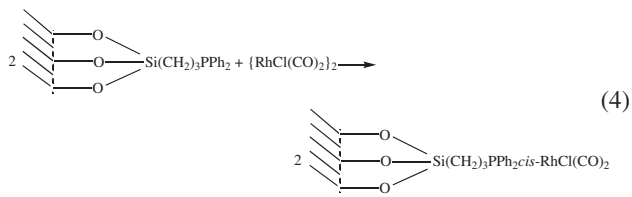

(4)

MCM-41(SH) reacts with $[\{RhCl(CO)_2\}_2]$ to form the dominant product $[MCM\text{-}41\{SRh(CO)_2\}]_2$ and the minor product MCM-41{$SRh_2Cl(CO)_4$} via substitution of the chloride in the bridge by the thiol:

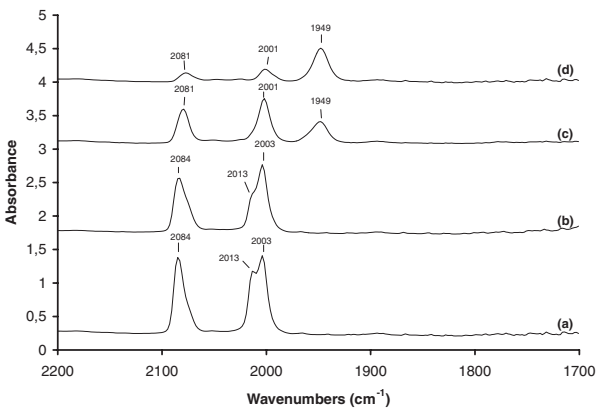

Fig. 2. IR spectra of the reaction mixtures. (a) Between $[\{RhCl(CO)_2\}_2]$ and 2 equiv of $[\{H_2N(CH_2)_3\}Si(OEt)_3]$ in *n*-hexane after 15 min; (b) Between $[\{RhCl(CO)_2\}_2]$ and 2 equiv of $[\{H_2N(CH_2)_3\}Si(OEt)_3]$ in *n*-hexane after 45 min; (c) Between $[\{RhCl(CO)_2\}_2]$ and 4 equiv of $[\{H_2N(CH_2)_3\}Si(OEt)_3]$ in *n*-hexane after 45 min; (d) Between $[\{RhCl(CO)_2\}_2]$ and 4 equiv of $[\{H_2N(CH_2)_3\}Si(OEt)_3]$ in *n*-hexane after 1 h 50 min.

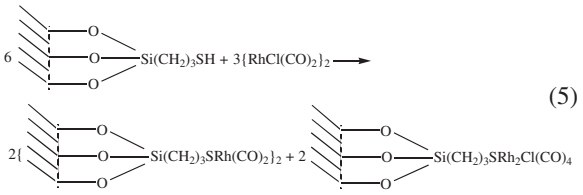

(5)

(b) By X-ray Diffraction: Figures 3, 4, and 5 show the XRD patterns of MCM-41-based powdered samples. The XRD spectrum of unfunctionalized MCM-41 exhibits an intense diffraction peak at a low angle ($2\theta = 2.16^\circ$) representing the d_{100} reflection line and two additional weak diffraction peaks at higher angles ($2\theta = 3.80^\circ$ and 4.36°) representing the d_{200} and d_{210} reflection lines, consistent with the characteristics of standard MCM-41.[23] Rh/MCM-41 had a XRD spectrum characteristic of MCM-41 with peak intensities comparable to those for unfunctionalized MCM-41. This demonstrates that the direct deposition of Rh on the channel walls of MCM-41 from $[\{RhCl(CO)_2\}_2]$ leads to no change in the mesoporous structure of MCM-41 without the involvement of a chemical reaction between $[\{RhCl(CO)_2\}_2]$ and the silanol groups of MCM-41. Meanwhile it should be considered that a deposited amount of Rh as low as 2% on MCM-41 may negligibly affect the mesoporous structure. After silylation of MCM-41, the XRD spectra of the resulting MCM-41(Cl), MCM-41(NH_2), and MCM-41(SH) obviously displayed a decreased peak intensity. Accordingly, it may be assumed that silylation of MCM-41 channels somewhat reduces mesopore size uniformity, but does not substantially alter the mesoporous structural ordering. When Cl was replaced with PPh_2 in MCM-41(Cl), the XRD peak intensities of the resulting MCM-41(PPh_2) continued to diminish. This may be due to the presence of larger PPh_2 ligands in the MCM-41 channels which further reduces mesopore size uniformity. Grafting of Rh on the three functionalized MCM-41 samples from $[\{RhCl(CO)_2\}_2]$ resulted in a small decrease in XRD spectral intensity, as shown in Figs. 4 and 5, probably because of the small amount of Rh coordinating with the functional groups.

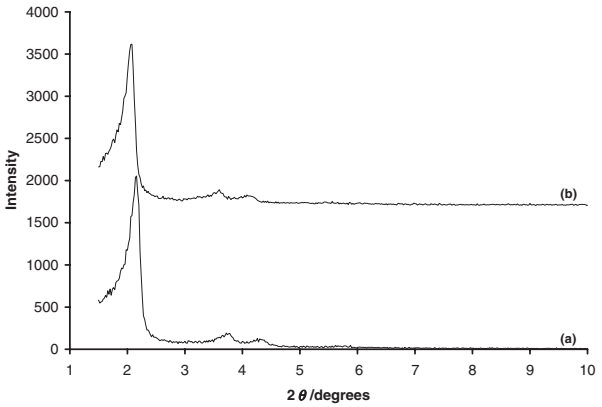

Fig. 3. XRD patterns of (a) MCM-41; (b) Rh/MCM-41.

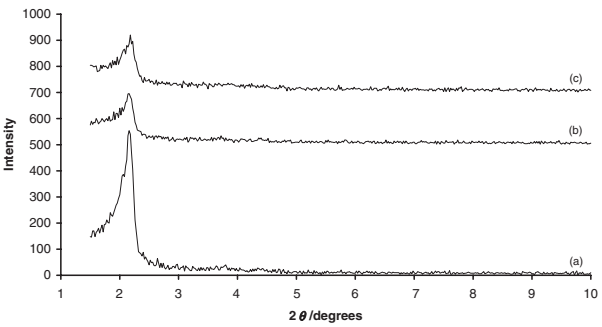

Fig. 4. XRD patterns of (a) MCM-41(Cl); (b) MCM-41(PPh_2); (c) Rh/MCM-41(PPh_2).

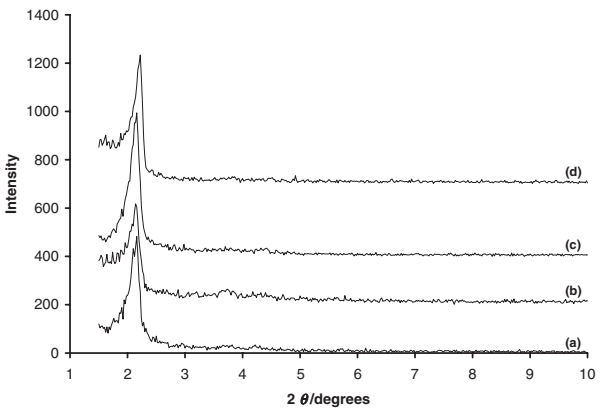

Fig. 5. XRD patterns of (a) MCM-41(NH_2); (b) Rh/MCM-41(NH_2); (c) MCM-41(SH); (d) Rh/MCM-41(SH).

(c) By N_2 Adsorption–Desorption: Figures 6, 7, and 8 show the N_2 adsorption–desorption isotherms of MCM-41-based powdered samples. Based on the N_2 adsorption branch data, the pore sizes, total pore volumes and BET surface areas were obtained (Table 1). Our unfunctionalized MCM-41 sample displayed typical type IV mesoporous adsorption–desorption behavior, agreeing with the known standard N_2 adsorption–desorption isotherm of MCM-41.[23] The uniform MCM-41 mesopores led to a narrow pore size distribution having a pore diameter (D_{BJH}) around 30 Å. Rh/MCM-41 gave a similar type IV mesoporous adsorption–desorption isotherm and a narrow pore size distribution, although its capillary condensation step emerged at slightly lower relative pressure. Deposition of Rh on MCM-41 caused only a weak reduction of the mean pore diameter from 30 to 28 Å and slight decreases of pore volume and surface area, probably because of the small amount of

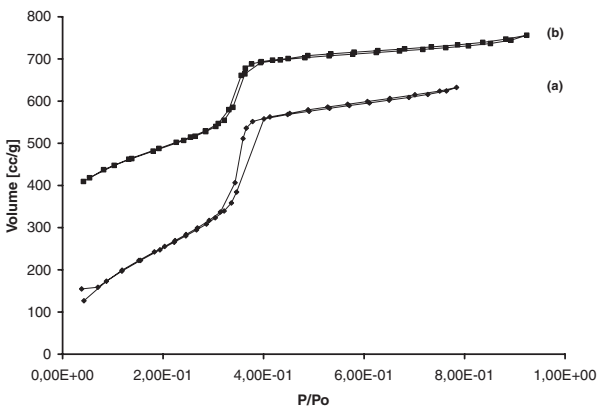

Fig. 6. N_2 adsorption–desorption isotherms of (a) MCM-41; (b) Rh/MCM-41.

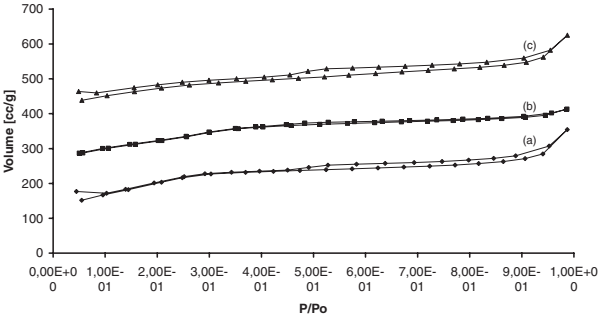

Fig. 7. N_2 adsorption–desorption isotherms of (a) MCM-41(Cl); (b) MCM-41(PPh_2); (c) Rh/MCM-41(PPh_2).

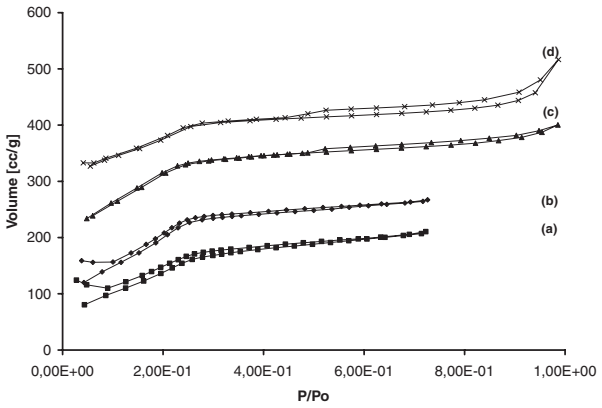

Fig. 8. N_2 adsorption–desorption isotherms of (a) MCM-41(NH_2); (b) Rh/MCM-41(NH_2); (c) MCM-41(SH); (d) Rh/MCM-41(SH).

Table 1. Physical Properties of Unfunctionalized and Functionalized MCM-41

Sample	Pore diameter /Å	Total pore volume /$cm^3\ g^{-1}$	BET surface area /$m^2\ g^{-1}$
MCM-41	30	1.29	1651
Rh/MCM-41	28	1.12	1568
MCM-41(Cl)	19	0.48	712
MCM-41(PPh_2)	18	0.31	460
Rh/MCM-41(PPh_2)	<18	0.35	421
MCM-41(NH_2)	19	0.43	726
Rh/MCM-41(NH_2)	22	0.33	762
MCM-41(SH)	24	0.78	1487
Rh/MCM-41(SH)	24	0.73	1415

Rh dispersed on the mesoporous channel walls. In contrast, MCM-41(Cl), MCM-41(NH_2), and MCM-41(SH) prepared by silylation showed adsorption–desorption isotherms with the capillary condensation steps obviously shifting to lower relative pressures and pore size distributions shifting to smaller pore diameters. Functionalization of MCM-41 resulted in not only an important reduction of mean pore diameter but remarkable decreases of pore volume and surface area. Therefore, the observed adsorption–desorption isotherms that deviated from that of MCM-41 may be interpreted in terms of stronger pore filling, given the organosilanes have larger chemical ligands. The replacement of Cl with PPh_2 produced further decreases in these parameters. The observed changes correlate with the organosilane's size. The greater change took place with ($[\{PH_2P(CH_2)_3\}Si(OMe)_3]$ which has a larger size. However, introduction of Rh to the mesopore channels by complexation with phosphine, amine, and thiol ligands led to little modification of the properties of N_2 adsorption–desorption due to the limited amount of Rh used.

2. Studies of Catalytic Cyclohexene Hydroformylation. All the catalyst precursors studied were tested for cyclohexene hydroformylation activity. Table 2 presents the comparative catalytic results at the end of a 20 h reaction over for each catalyst system. The blank test showed no catalytic activity in the autoclave. All the catalysts displayed selectivities greater than 98% to cyclohexane carboxaldehyde with no formation of alcohols under the reaction conditions.

When $[\{RhCl(CO)_2\}_2]$/MCM-41(NH_2) was used as a catalyst precursor, a turnover of 2091 (mol/mol Rh) of converted cyclohexene was obtained in the first reaction cycle, 99.4% of which was hydroformylated to cyclohexane carboxaldehyde and only 0.6% of which was hydrogenated to cyclohexane. This catalytic performance prevails over that of a homogeneous catalyst derived from $[\{RhCl(CO)_2\}_2]$. When a reaction cycle of 20 h ended, the solid sample was filtered off from the reaction mixture in air. After the first cycle, the solid sample color remained yellow and the liquid phase color turned light yellow. According to the results of the elemental analysis (Table 3), 1.59% of Rh was retained on the solid sample. This accounts for a weak loss of surface amine ligand bonded rhodium catalytic components from the support, referring to the initial rhodium loading of 1.88% during the first cycle. In the second cycle, the catalytic hydroformylation activity was noted to slightly decrease due to the slight loss of catalytic components from the support during the first cycle. The solid sample color still remained yellow and the liquid phase was colorless after the reaction. Simultaneously, the rhodium content of the solid sample did not markedly diminish. In the third and fourth cycles, the catalytic hydroformylation activity was found to significantly increase with no change in rhodium content of the solid sample. The results demonstrate that the MCM-41(NH_2)-tethered catalyst is substantially stable for recycling as well as active in cyclohexene hydroformylation, owing to the proper coordinative bonding between the surface amine and the rhodium centre.

Table 2. Catalytic Properties of $[\{RhCl(CO)_2\}_2]$-Derived Catalysts[a] in Cyclohexene Hydroformylation[b]

Catalyst precursor	Cyclohexene conversion /%	Turnover[c] (mol/mol Rh)	Product distribution/mol%	
			Cyclohexane	Cyclohexane carboxaldehyde
$[\{RhCl(CO)_2\}_2]$[d]	59.4	1131	0.8	99.2
$[\{RhCl(CO)_2\}_2]$/MCM-41(NH_2)				
1st cycle	96.6	2091	0.6	99.4
2nd cycle	80.4	2058	0.5	99.5
3rd cycle	94.1	2439	0.8	99.2
4th cycle	95.5	2476	0.8	99.2
$[\{RhCl(CO)_2\}_2]$/MCM-41(PPh_2)				
1st cycle	93.9	2011	1.6	98.4
2nd cycle	3.6	1832	0.3	99.7
$[\{RhCl(CO)_2\}_2]$/MCM-41(SH)	0	—	—	—

a) 0.30 g of catalyst precursor with nearly 2.0% Rh loading; b) Reaction conditions: 28 bar, 100 °C, $H_2/CO = 1$, 20 h per cycle; c) For conversion of cyclohexene; d) 0.012 g.

Table 3. Color and Rhodium Content Changes of Supported Rhodium Complex Samples before and after Cyclohexene Hydroformylation

Catalyst precursor	Before reaction		After reaction	
	Color	Rh/%	Color	Rh/%
$[\{RhCl(CO)_2\}_2]$/MCM-41(NH_2)				
1st cycle	Yellow	1.88	Yellow	1.59
2nd cycle	Yellow	1.59	Yellow	1.57
3rd cycle	Yellow	1.57	Yellow	1.57
4th cycle	Yellow	1.57	Yellow	1.57
$[\{RhCl(CO)_2\}_2]$/MCM-41(PPh_2)	Brown	1.90	Light yellow	0.08
$[\{RhCl(CO)_2\}_2]$/MCM-41(SH)	Yellow	1.90	Yellow	1.90

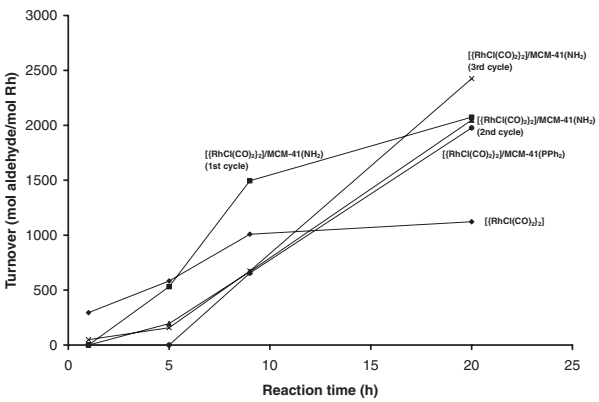

Fig. 9. Turnovers of cyclohexane carboxaldehyde formed as a function of reaction time over $[\{RhCl(CO)_2\}_2]$-derived catalysts.

The observations of the increased catalytic activities in the third and fourth cycles are not understood for the time being. The increased turnover values are significant according to our experimental error. A similar phenomenon has been observed in cyclohexene hydroformylation with $\{RhH(CO)(PPh_3)_3\}/SiO_2$-(SH).[24] Under catalytic conditions, a catalyst precursor must undergo an induction period prior to becoming an active species. It can be seen from Fig. 9 that a longer induction time is required for the tethered catalyst precursor $[\{RhCl(CO)_2\}_2]$/MCM-41(NH_2) than for the homogeneous catalyst precursor $[\{RhCl(CO)_2\}_2]$. Namely, the former is converted to an active species under hydroformylation conditions more slowly than the latter. This leads us to assume the possibility that the amount of active species derived from $[\{RhCl(CO)_2\}_2]$/MCM-41(NH_2) increases progressively as the reaction proceeds. Hence, the catalytic activity may increase with an increasing amount of the active species.

By contrast, although $[\{RhCl(CO)_2\}_2]$/MCM-41(PPh_2) led to a turnover of 2011 (mol/mol Rh) for cyclohexene conversion in the first reaction cycle, a heavy rhodium leaching occurred during the reaction. After the first cycle, the solid sample color turned light yellow and the liquid phase color became brown. The light yellow solid sample contained only 0.08% of Rh, referring to the initial rhodium loading of 1.90%, so that the conversion of cyclohexene declined to 3.6% in the second cycle. The results show that the surface phosphine disfavors the immobilization of the rhodium complex in cyclohexene hydroformylation. In the case of $[\{RhCl(CO)_2\}_2]$/MCM-41(SH), neither catalytic activity nor leaching of the rhodium species were detected, as seen in Tables 2 and 3. This implies that the surface thiol cannot activate the rhodium complex for cyclohexene hydroformylation via the strong coordinative bonding with the rhodium centre.

Figure 9 illustrates the variation of turnovers of cyclohexane carboxaldehyde formed on these catalyst systems with reaction time. All the supported catalyst systems maintained hydroformylation activity throughout 20 h of reaction as their turnovers of aldehyde formed increased continuously with reaction time.

In the first hour, the homogeneous [{$RhCl(CO)_2$}$_2$] system was the most active and all the supported catalyst systems were little active. Then the activity of the former decreased but its turnover still increased with reaction time till 9 h of total time, whereas the activities of the supported catalyst systems increased gradually. After 9 h, the homogeneous [{$RhCl(CO)_2$}$_2$] system was almost not active. At the same time, the reaction solution changed from yellow to colorless in color, with the concomitant formation of black precipitate, which was indicative of the metallic aggregation from [{$RhCl(CO)_2$}$_2$] under pressurized ($CO + H_2$). This phenomenon did not occur with the supported catalyst systems. The turnover of aldehyde formed on [{$RhCl(CO)_2$}$_2$]/MCM-41(NH_2) increased linearly with reaction time from the second reaction cycle. This indicates that the MCM-41(NH_2)-tethered catalyst can maintain its activity unchanged in a prolonged reaction.

The catalytic results demonstrate that the [{$RhCl(CO)_2$}$_2$]/MCM-41(NH_2)-derived catalyst is not only highly active but quite stable for recycling. These results also demonstrate that the [{$RhCl(CO)_2$}$_2$]/MCM-41(SH)-derived catalyst is inactive though very stable, and that the [{$RhCl(CO)_2$}$_2$]/MCM-41(PPh_2)-derived catalyst suffers from heavy rhodium leaching. The [{$RhCl(CO)_2$}$_2$]/MCM-41(NH_2)-derived catalyst which has good performances, exhibits obvious advantages over the [{$RhCl(CO)_2$}$_2$]-derived homogeneous catalyst in both activity and stability. Among the three tethered catalysts via different donor ligands, the [{$RhCl(CO)_2$}$_2$]/MCM-41(SH)-derived catalyst is the most resistant to rhodium leaching, and the [{$RhCl(CO)_2$}$_2$]/MCM-41(PPh_2)-derived catalyst is the less resistant to rhodium leaching. The [{$RhCl(CO)_2$}$_2$]/MCM-41(NH_2)-derived catalyst also turns out to have much better resistance to rhodium leaching than the [{$RhCl(CO)_2$}$_2$]/MCM-41(PPh_2)-derived catalyst. This had not been clarified in the previous studies concerning 1-hexene hydroformylation with [{$RhCl(CO)_2$}$_2$]-derived SiO_2-tethered catalysts via donor ligands, as SiO_2{$PPh_2RhCl(CO)_2$} has never been compared with others.[5,6] It follows that the effect of donor ligands on the immobility of the rhodium complex has, from strongest to weakest –SH > $–NH_2$ > $–PPh_2$.

The strength of complexation of the supported donor ligands with the rhodium centre determines the catalytic properties of the tethered catalysts, along with their resistance to rhodium leaching. It is known that phosphine, amine, and thiol ligands are all strong σ-electron donors. In the meantime, $(O_s)_3$Si{$(CH_2)_3PPh_2$} and $(O_s)_3$Si{$(CH_2)_3SH$} (O_s: surface oxygen) are poor and strong π-electron acceptors, respectively. As a result, the weak dπ–pπ bonding between the phosphorus and the rhodium centre results in the transfer of the negative charge from the phosphorus to the rhodium complex in the case of MCM-41{PPh_2*cis*-$RhCl(CO)_2$}. This favors the formation of a hydridic complex necessary for hydroformylation by hydrogenolysis of the Rh–Cl bond under hydroformylation conditions, and thus renders the MCM-41{PPh_2*cis*-$RhCl(CO)_2$}-derived catalyst active. Meanwhile, the weak dπ–pπ bonding forms a weak P–Rh bond, so that a supported phosphine coordinated to the rhodium complex is readily replaced by CO with the occurrence of rhodium leaching under hydroformylation conditions. In the case of [{$RhCl(CO)_2$}$_2$]/MCM-41(SH), the strong dπ–pπ bonding leads to the transfer of the negative charge from the rhodium centre to the sulphur, which impedes the formation of an active hydridic complex by hydrogenolysis of the Rh–Cl bond under hydroformylation conditions. This renders the [{$RhCl(CO)_2$}$_2$]/MCM-41(SH) catalyst system inactive. In contrast, $(O_s)_3$Si{$(CH_2)_3NH_2$} has no dπ orbitals. However, a strong N–Rh bond may be formed and the transfer of the negative charge from the rhodium centre to other ligands can be controlled by the strong electronegativity of the nitrogen. It may be assumed that the presence of an amine ligand in the tethered complex helps the transformation of the Rh–Cl bond into the Rh–H bond proceed to a satisfactory extent. The complexation of a supported amine with [{$RhCl(CO)_2$}$_2$] not only produces a tight N–Rh bond to immobilize the complex, but ensures stable and high catalytic activity for hydroformylation.

The electronic effects of supported donor ligands on the catalytic activity and stability of a metallic carbonyl complex can also cause spectral variation in the vibration of carbonyl groups in the complex. An IR carbonyl spectral change does occur after [{$RhCl(CO)_2$}$_2$] has been tethered to MCM-41 via phosphine, amine, and thiol ligands in the forms of MCM-41{PPh_2*cis*-$RhCl(CO)_2$}, MCM-41{NH_2*cis*-$RhCl(CO)_2$} and [MCM-41{$SRh(CO)_2$}]$_2$ plus MCM-41{$SRh_2Cl(CO)_4$}. However, the spectral comparison is significant only for MCM-41{$PPh_2RhCl(CO)_2$} and MCM-41{$NH_2RhCl(CO)_2$} with respect to [{$RhCl(CO)_2$}$_2$]/MCM-41. The coordination of supported phosphine or amine results in the transfer of the increased negative charge to the carbonyls via the rhodium by π-back donation and thus the weakening of the C=O bond vibration. In fact, the gem-dicarbonyl bands at 2096 and 2017 cm^{-1} for MCM-41{$NH_2RhCl(CO)_2$} have a significant downward shift compared to those at 2113sh, 2098, and 2042 cm^{-1} for [{$RhCl(CO)_2$}$_2$]/MCM-41, as shown in Fig. 1. The gem-dicarbonyl bands at 2081 and 2003 cm^{-1} for MCM-41{PPh_2*cis*-$RhCl(CO)_2$} observed in our previous work show a stronger downward shift than those for MCM-41{$NH_2RhCl(CO)_2$}.[25] It is evident that both supported phosphine and supported amine donate their negative charge to the rhodium complex, but more negative charge is transferred to the carbonyls from supported phosphine than from supported amine. The IR observations are in accord with the above explanation regarding the influences of supported phosphine and amine ligands on the catalytic activity and stability of tethered rhodium complexes. The unavailability of MCM-41{$SHRhCl(CO)_2$} does not permit us to examine the shift of gem-dicarbonyl bands with supported thiols coordinated under identical conditions. Therefore, in order to demonstrate the electronic contributions of these ligands to a complex with regards to their promoting actions on catalytic activity and stability, we intend to study the trend in the carbonyl vibration in MCM-41-tethered rhodium monocarbonyl complexes via these ligands in complexes such as MCM-41{$PPh_2RhH(CO)(PPh_3)_2$}, MCM-41{$NH_2RhH(CO)(PPh_3)_2$} and MCM-41{$SHRhH(CO)(PPh_3)_2$}.

Finally, it is important to mention that the XRD spectrum of the [{$RhCl(CO)_2$}$_2$]/MCM-41(NH_2)-derived catalyst maintained the initial peak intensities for mesoporous MCM-41 after the fourth reaction cycle, as shown in Fig. 10. This demonstrates that the mesoporous structure of the MCM-41-based catalysts is not affected by operating catalytic conditions.

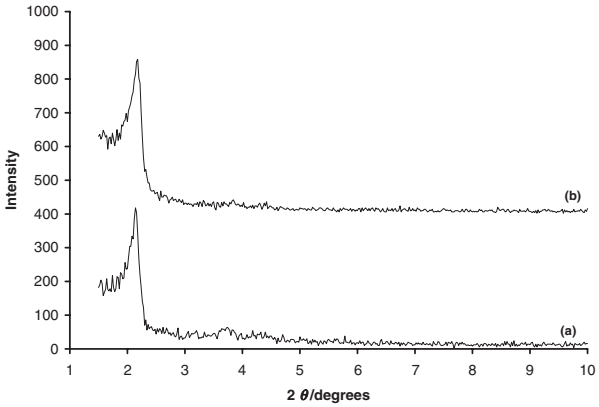

Fig. 10. XRD patterns of (a) fresh [{RhCl(CO)$_2$}$_2$]/MCM-41(NH$_2$) and (b) [{RhCl(CO)$_2$}$_2$]/MCM-41(NH$_2$) after four cyclohexene hydroformylation cycles (80 h) at 28 bar of (CO + H$_2$) and at 100 °C.

Conclusions

[{RhCl(CO)$_2$}$_2$]-derived rhodium complexes have been anchored to MCM-41(PPh$_2$), MCM-41(NH$_2$), and MCM-41(SH). On MCM-41(NH$_2$), the reaction of [{RhCl(CO)$_2$}$_2$] with the amine is found to give MCM-41{NH$_2$*cis*-RhCl(CO)$_2$} by splitting of the chloride bridge. On MCM-41(PPh$_2$) and on MCM-41(SH), it is inferred by analogy with the known reactivities of [{RhCl(CO)$_2$}$_2$] on SiO$_2$(PPh$_2$) and on SiO$_2$(SH) that [{RhCl(CO)$_2$}$_2$] reacts with the donor ligands to form MCM-41{PPh$_2$*cis*-RhCl(CO)$_2$}, [MCM-41{SRh(CO)$_2$}]$_2$ and MCM-41{SRh$_2$Cl(CO)$_4$}. The tethering of rhodium complexes does not alter the structural ordering of MCM-41, while it results in reduced pore sizes, pore volumes, and BET surface areas.

All of the [{RhCl(CO)$_2$}$_2$]-derived catalysts studied possess very high selectivity (>98%) to cyclohexane carboxaldehyde in cyclohexene hydroformylation at 28 bar of equimolar CO and H$_2$ and at 100 °C. The homogeneous [{RhCl(CO)$_2$}$_2$]-derived catalyst readily deactivates during the reaction due to the reduction of [{RhCl(CO)$_2$}$_2$] to rhodium metallic particles under a pressurized reducing atmosphere. The [{RhCl(CO)$_2$}$_2$]/MCM-41(NH$_2$)-derived catalyst is not only the most active but quite stable for recycling. Only limited rhodium leaching is observed after three reaction cycles. The [{RhCl(CO)$_2$}$_2$]/MCM-41(PPh$_2$)-derived catalyst easily loses the rhodium during reaction. The [{RhCl(CO)$_2$}$_2$]/MCM-41(SH)-derived catalyst is the most resistant to rhodium leaching but inactive. The distinction in the catalytic behavior and stability is attributable to the strength of interaction of the supported donor ligands with the rhodium centre. The complexation of a supported amine with [{RhCl(CO)$_2$}$_2$] produces a tight N–Rh bond, and does not influence the transformation of the Rh–Cl bond into an active hydridic complex under hydroformylation conditions. The [{RhCl(CO)$_2$}$_2$]/MCM-41(NH$_2$)-derived catalyst is of marked advantage in activity, stability and recovery in hydroformylation.

The mesoporous structure of MCM-41 in the catalysts is maintained unchanged under operating reaction conditions in this work.

References

1 M. Lenarda, L. Storaro, and R. Ganzerla, *J. Mol. Catal. A: Chem.*, **111**, 203 (1996), and references therein.
2 A. Sayari, *Chem. Mater.*, **8**, 1840 (1996).
3 A. Corma, *Chem. Rev.*, **97**, 2373 (1997).
4 K. G. Alum, R. D. Hancock, I. V. Howell, S. Mckenzie, R. C. Pitkethly, and P. J. Robinson, *J. Organomet. Chem.*, **87**, 203 (1975).
5 R. D. Hancock, I. V. Howell, R. C. Pitkethly, and P. J. Robinson, "Catalysis: Heterogeneous and Homogeneous," ed by B. Delmon and G. James, Amsterdam (1975), pp. 361–371.
6 K. G. Allum, R. D. Hancock, I. V. Howell, S. Mckenzie, R. C. Pitkethly, and P. J. Robinson, *J. Catal.*, **43**, 322 (1976).
7 H. Arai, *J. Catal.*, **51**, 135 (1978).
8 H. Schumann, G. Gielusek, S. Jurgis, E. Hahn, J. Pickardt, J. Blum, Y. Sasson, and A. Zoran, *Chem. Ber.*, **117**, 2825 (1984).
9 M. Eisen, T. Bernstein, J. Blum, and H. Schumann, *J. Mol. Catal.*, **43**, 199 (1987).
10 Ph. Kalck and F. S. Spirau, *New J. Chem.*, **13**, 515 (1989).
11 H. Gao and R. J. Angelici, *Organometallics*, **17**, 3063 (1998).
12 H. Gao and R. J. Angelici, *New J. Chem.*, **23**, 633 (1999).
13 H. Gao and R. J. Angelici, *J. Mol. Catal. A: Chem.*, **149**, 63 (1999).
14 H. Gao and R. J. Angelici, *J. Mol. Catal. A: Chem.*, **145**, 83 (1999).
15 H. Gao and R. J. Angelici, *Organometallics*, **18**, 989 (1999).
16 M. Eisen, J. Blum, H. Schumann, and S. Jurgis, *J. Mol. Catal.*, **31**, 317 (1985).
17 M. Nowotny, T. Maschmeyer, B. F. G. Johnson, P. Lahuerta, J. M. Thomas, and J. E. Davies, *Angew. Chem., Int. Ed.*, **40**, 955 (2000).
18 J. L. Bilhou, V. Bilhou-Bougnol, W. F. Graydon, J. M. Basset, A. K. Smith, G. M. Zanderighi, and R. Ugo, *J. Organomet. Chem.*, **153**, 73 (1978).
19 D. N. Lawson and G. Wilkinson, *J. Chem. Soc.*, **1965**, 1900.
20 R. Ugo, F. Bonati, and M. Fiore, *Inorg. Chim. Acta*, **2**, 463 (1968).
21 L. D. Rollman, *Inorg. Chim. Acta*, **6**, 137 (1972).
22 J. A. McCleverty and G. Wilkinson, *Inorg. Synth.*, **8**, 211 (1966).
23 J. S. Beck, J. C. Vartuli, W. J. Roth, M. E. Leonowicz, C. T. Kresge, K. D. Schmitt, C. T.-W. Chu, D. H. Olson, E. W. Sheppard, S. B. McCullen, J. B. Higgins, and J. L. Schlenker, *J. Am. Chem. Soc.*, **114**, 10834 (1992).
24 L. Huang and S. Kawi, *Catal. Lett.*, in press.
25 A. M. Liu, K. Hidajat, and S. Kawi, *J. Mol. Catal. A: Chem.*, **168**, 303 (2001).